CDF/ANAL/EXOTIC/CDFR/7261
Version 2.1
April 10, 2008

Background Estimation for the High-p_T Like-Sign Dilepton Analysis to Search for the Wh Production

Toru Okusawa, Yoshihiro Seiya, Takayuki Wakisaka, and Kazuhiro Yamamoto
Osaka City University, Japan

Abstract

This note describes the background estimation for our fermiophobic higgs and high-mass Standard-Model higgs searches using like-sign dilepton (ee, $e\mu$, and $\mu\mu$) events. Although our main analysis deals with like-sign dilepton events, the studies presented in this note include opposite-sign dilepton events as well to understand the overall like-sign analysis better. Moreover, we do not introduce any detailed tunings of additional dilepton selections specific to the higgs search at this stage of studies, but try to investigate background events for fairly generic dilepton events. The physics backgrounds containing prompt real-leptons are estimated by Monte Carlo samples, while fake-lepton backgrounds and residual photon-conversion backgrounds are estimated by data-driven methods. The studies starts from looking at the least-biased dilepton events which are simply isolated dilepton events of good-quality and are satisfying our asymmetric p_T cut with the high-p_T cut at 20 GeV/c and the low-p_T cut at 6 GeV/c. We then gradually proceed to investigations with more restricted event selections. Additional biases considered in this note include a Z veto. The discussion also extends to the case where all the lepton tracks are required to have silicon hits to reduce mainly the residual conversions. The sample with the silicon-hit requirement will be used in our final analysis for the higgs searches. For these events, we further look into comprehensive comparisons between the data and our background expectations on the 2 dimentional plane of the 2nd lepton p_T and the p_T of dilepton system by computing integrated number of events as a function of cut values on the two p_T's. As a conclusion, we do not see any significant discrepancies between the observed data and the background expectation.

1 Introduction

Our physics objective is to search for the low-mass fermiophobic higgs and the high-mass Standard-Model (SM) higgs boson using like-sign (LS) dilepton events produced by

$$qq' \to W^{\pm}h \to W^{\pm}W^{*}W^{*} \to \ell^{\pm}\ell^{\pm} + X \ , \tag{1}$$

where the leptonic decay of two W bosons with the same electric charge makes the LS dilepton final state. Although the LS requirement is quite effective to suppress QCD and known electroweak processes, we expect that the fake-lepton backgrounds and residual photon-conversions, which are photon conversions with unobserved partner tracks thus escaping a conversion-veto, still remain at a considerable level in the events of our signature, which was in fact confirmed by the previous analysis [1, 2].

In the updated studies described in this note, we expand our analysis to include the data corresponding to an integrated luminosity of about 2 fb^{-1}. The baseline selection for the updated analysis, essentially the same as before though, is given in [3]. Briefly, we apply an asymmetric kinematical cut, where the high-p_T cut is 20 GeV/c and the low-p_T cut is 6 GeV/c, an isolation cut, lepton identification cuts, and a couple of simple cuts on dilepton pairs. The events are required to have exactly two good-lepton candidates, and multi-lepton events more than two leptons are excluded from the baseline sample. Any other cuts such as charge combination, Z vetoes, missing E_T etc. are not required, which results in 54454 events found in the data. Our convention is to distinguish $e\mu$ and μe events in a way such that the first lepton has a higher p_T value[1]. As before, the fake-lepton backgrounds and the residual photon-conversions are estimated by data-driven methods, while other backgrounds containing prompt real-leptons (physics backgrounds) are estimated by Monte Carlo (MC) data. Some technical aspects of the bases for the estimation of residual photon-conversions and fake-lepton backgrounds are changed, which are described in [4] and [5], respectively. The scale factors (SF) to be applied to the MC data are obtained in [6].

The overall structure of this note is to start looking at the baseline dilepton events and generally proceed to more biased samples but without introducing any specific cuts for the higgs searches. Concretely, we investigate

1. baseline dileptons of the opposite-sign (OS) pairs,
2. the OS dileptons after a Z veto,
3. baseline dileptons of the LS pairs,
4. the LS dileptons after the Z veto.

We then repeat similar analyses with requiring silicon hits for tracks as a track-quality cut mainly to further reduce residual-conversion backgrounds. Since the LS dilepton events with the silicon-hit requirement are the sample that we deal with in the final

[1] We use the track p_T for electrons too for the lepton ordering.

analysis, we look into more detailed comparisons between the observed data and background expectations on the 2 dimensional plane of the 2nd lepton p_T vs. the p_T of dilepton system.

2 Background esimation

2.1 Residual photon-conversions

Since the details of the method for estimating residual photon-conversions are described in [4], we only briefly review them. The amount of residual conversion backgrounds is estimated from the rate of identified photon conversions by multiplying appropriate weights that connect the yields of identified conversions and residual conversions. These weights are expressed in terms of the detection efficiency for conversions $\varepsilon_{\mathrm{con}}$ as

$$R_{\mathrm{res}} = \frac{1 - \varepsilon_{\mathrm{con}}}{\varepsilon_{\mathrm{con}}} \,. \tag{2}$$

What we have to know is then basically the number of identified conversions. Complications from the fact that the $\varepsilon_{\mathrm{con}}$ is not a constant but be parametrized are worked out and described in [4]. The estimation of residual conversions is therefore to sum up R_{res} event by event.

For the dilepton analysis, we collect events with exactly one good lepton satisfying our high-p_T ($p_T > 20$ GeV/c) lepton selection and look for additional photon conversions in the events passing our low-p_T ($E_T > 6$ GeV and $p_T > 6$ GeV/c) electron selection except the conversion-veto. The first lepton (the lepton of the high-p_T side) is actually a lepton candidate (ℓ') and would consist of real-lepton (ℓ), fakes (f), and residual conversions (c). This can be symbolically expressed by

$$\ell' \equiv \ell + f + c \,. \tag{3}$$

The lepton + residual conversions are then written by

$$\ell' c = (\ell + f + c)c = \ell c + f c + cc \,. \tag{4}$$

On the other hand, we realize through various investigations that there are non-negligible contributions of events in which the 1st lepton is a conversion electron and the 2nd lepton is a prompt lepton. In order to take these backgrounds into account, we also estimate the residual conversions of the type $c\ell'$, that is,

$$c\ell' = c(\ell + f + c) = c\ell + cf + cc \,. \tag{5}$$

By comparing this with Eq. (4), we identify a double count of cc backgrounds in this scheme. There is actually another double count of the type cf because we separately estimate fake-lepton backgrounds from lepton + isolated track events:

$$\ell' f = (\ell + f + c)f = \ell f + ff + cf \,. \tag{6}$$

These double counts, cc and cf, are subtracted by explicitly collecting conversion + conversion events and conversion + track events with multiplying appropriate weights in the same way as nominal residual-conversion and fake-lepton estimation[2]. We note that resulting values of residual-conversion estimation could even become negative, especially when they are small, depending on the statistical fluctuation due to the subtraction.

2.2 Fake leptons

Fake-lepton backgrounds are estimated from the number of events with one good lepton candidate passing the high-p_T cut plus isolated tracks by multiplying appropriate weights (fake rates). The "fake lepton" here is a generic word including non-prompt leptons such as coming from (semi-)leptonic decays of heavy-flavor hadrons as well as literal fake leptons. The exact definition of the denominator objects (the isolated tracks) to define the fake rates is described in [5]. Quickly, it is an isolated track passing the low p_T cut, a set of track-quality cuts, and the requirements on the energy depositions in the corresponding calorimeter towers, which we refer to as hadronic tracks. The cuts on the energy deposition have no overlap with the nominal lepton selection, thus the hadronic tracks are fake-enriched objects. The fake rates are obtained as a function of track p_T and the actual numbers are obtained from generic jet samples.

2.3 Monte Carlo samples

The physics backgrounds can be classified into reducible and irreducible backgrounds:

- Reducible backgrounds
    1. $Z/\gamma^* \to \ell^+\ell^-$,
    2. W+(heavy-flavor hadrons)$\to \ell\ell + X$,
    3. $t\bar{t} \to (W^+b)(W^-\bar{b}) \to \ell\ell + X$,
    4. $W^+W^- \to (\ell^+\nu)(\ell^-\nu)$.
- Irreducible backgrounds
    1. $WZ \to (\ell^\pm\nu)(\ell^+\ell^-)$,
    2. $ZZ \to (\ell^+\ell^-)(\ell^+\ell^-)$,

The reducible backgrounds are reduced first of all by the LS requirement. When they contribute to LS dilepton events, the events are most likely due to residual conversions or fake leptons contained in these physics events, thus reduced also by the isolation cut. The irreducible backgrounds are suppressed mainly by a Z veto at the first order.

[2] Up to the current stage of our analysis, we have not detected any signs of considerable contributions of events of the type $f\ell'$ in which the isolated track has a larger p_T than the identified good lepton candidates.

The MC samples were produced by the Electroweak and the Top groups. Table 1 lists the MC samples and related information of them. The MC data are all applied with the relevant scale factors that are discussed in [6]. A rather important point regarding our MC prediction is that residual photon-conversions and fake-leptons including non-prompt leptons from (semi-)leptonic decays of heavy-flavor hadrons found in the MC events are explicitly removed from the MC contributions by looking at the `OBSP` information since their contributions are assumed to be directly estimated from the data-driven methods.

3 Opposite-sign dilepton events

Figure 1 shows a comparison of the 2nd lepton E_T or p_T distributions between the data and the background expectation. The background components in the legend of the plot are shown from the largest contributions and only for the backgrounds with non-zero yields. The uncertainty in the plot as a hatch represents the total uncertainty of the background expectation including statistical uncertainty and the uncertainty of the SFs, but the uncertainty of the integrated luminosity (6%) is not included since it is a normalization uncertainty and not specific to a given bin. The details of event counting is summarized in Table 2. In the table, there are numbers denoted by +0.0 and 0.0. The +0.0 means that naive event counting shows non-zero contribution but they are eventually removed or reduced to some values less than the precision shown in the table by the filtering of MC fake-leptons at the `OBSP` level, while the 0.0 indicates exactly no event passing the event selection.

The next step is to apply a Z veto. The Z veto is already used in our analysis when we estimate fake-rates using jet samples as described in [5] in order to remove real leptons from the Drell-Yan processes. The veto here is introduced in a different context aiming mainly to reduce WZ backgrounds which are irreducible in our channel, but the method itself is basically the same, which we briefly repeat here. For each lepton identified with our selection, the algorithm looks for a high-p_T isolated track with oppositely charged or a loosely-identified lepton of the same type but without asking charge combination, and discards the event if the invariant mass falls in a Z mass window between 81 GeV/c^2 and 101 GeV/c^2. The choice of these Z-leg objects represents efforts to widen the acceptance of Z legs, including plug electrons for example, to catch Z events as many as possible. The detailed criteria for identifying such Z-leg objects is given in [5]. Figure 2 shows the 2nd lepton E_T or p_T distributions after the Z veto, and Table 3 is the details of event counting.

4 Like-sign dilepton events

Similar results for the LS events are obtained. Figure 3 shows the 2nd lepton E_T or p_T distributions before the Z veto, while Fig. 4 corresponds to the case after applying the Z veto. The application of Z removal to LS lepton-pairs, dielectrons particularly, rejects contributions originally from OS pairs but eventually turning out to be LS pairs due to the LS tracks from conversions of collinear hard-photons emitted off the lepton, the so-called "tridents". Tables 4 and 5 summarize the details of event counting before and after the Z veto, respectively.

5 Requiring silicon hits

We repeat the analysis with requiring silicon hits for tracks as a track-quality cut mainly to reduce residual photon-conversions:

$$\text{the number of Si hits} \geq 3\,. \tag{7}$$

Figure 5 shows the 2nd lepton E_T or p_T distributions before the Z veto, while Fig. 6 shows the distributions after the Z veto. The results for the LS events are shown in Fig. 7 before the Z veto, and in Fig 8 after the Z veto. The details of the event counts are listed in Tables 6 and 7 for the OS events, and Tables 8 and 9 for the LS events. The data and the background expectations are in good agreements.

We further investigate details of the LS dilepton events. In the original analysis [2], we examined the LS events on the 2 dimentional plane of the 2nd lepton p_T (p_{T2}) and the p_T of dilepton system (p_{T12}). For a given set of cut values on the p_{T2} and the p_{T12}, we can divide the 2 dimentional plane into 4 regions. We call the upper left the region 1, the lower left the region 2, the lower right the region 3, and the upper right the region 4. We then chose the region 4 to obtain the final cross section limit.

Here, we perform a thorough comparison on this plane between the data and the background predictions by using the integrated number of events in each region, repeating the computation with scanning the cut values on the two p_T's, and filling the results into 2 dimentional histograms as a function of cut values. The comparison is expressed in terms of the significance, we thus obtain 4 values of the significance for a given set of cut values.

The significance is derived from the so-called p value. Our construction of the p value is motivated to quantify inconsistencies between the data and the background expectations in terms of not only excesses but also deficits. The p-value calculation is performed in the framework of the prior-predictive method [7], i.e. the observed number of events is modeled by the Poisson statistics multiplied by the background prior with integrating nuisance parameters out. We use the truncated Gaussian as the background prior, then the probability density function (PDF) of the observed number of events is given by

$$\mathcal{P}(n|B, \Delta B) = \int_0^{+\infty} db \frac{e^{-b} b^n}{n!} \tilde{G}(b|B, \Delta B)\,, \tag{8}$$

where $\tilde{G}(b|B, \Delta B)$ represents a truncated Gaussian with the mean B and the sigma ΔB. When the observed number of events is given by n_0, we first compute the usual

p value with the test statistic n by

$$p = \sum_{n=n_0}^{+\infty} \mathcal{P}(n|B, \Delta B) . \tag{9}$$

If this p is larger than 0.5, we investigate the shortage of the observed number of events by

$$p = \sum_{n=0}^{n_0} \mathcal{P}(n|B, \Delta B) . \tag{10}$$

If this p is still larger than 0.5, we set $p = 0.5$. Then, we use one-sided conversion of the p value to the sigma s:

$$p = 1 - \mathrm{Freq}(s) , \tag{11}$$

where the Freq(x) is the frequency function defined by

$$\mathrm{Freq}(x) \equiv \frac{1}{\sqrt{2\pi}} \int_{-\infty}^{x} dt \; e^{-\frac{t^2}{2}} . \tag{12}$$

The sign of s is assigned to be positive for the usual p value and negative for the lower side integration of the PDF. Figure 9 shows the results of comparisons in terms of the significance, while Figs. 10 and 11 show the number of LS dilepton events and the background expectations, respectively, integrated in each region as a function of cut values on the p_{T2} and p_{T12} to know the level of the absolute statistics at each point. We see some scatters of spots with the significance close to or a little greater than 2, which are probably due to staistical fluctuation because the regions are small and well correlated with the binning structure. Overall, we conclude that agreements between the data and background predictions are good in every aspect on this 2 dimentional plane.

6 Conclusions

We compared the dilepton events, both the opposite-sign and like-sign pairs, between the data and the full background predictions. The data and predictions are in good agreement before and after the Z veto. The consistency was checked in details on the 2 dimensional plane of the 2nd lepton p_T and the dilepton-system p_T with changing the cut values on these p_T values. Again, we did not find any significant excess in the data with respect to the background predictions.

Table 1: Summary of the Monte Carlo samples.

Process	Datasets	Events	$\sigma \cdot B_F$ (pb)	K factor	Filter-efficiency	Luminosity (fb^{-1})	Notes
Electron channels							
$W \to e\nu$	`wewkge`	4036290	1960	1.4	—	1.47	
$Z/\gamma^* \to ee$	`zewkad`	1594110	355 ± 3	1.4	—	3.21	$M > 20$ GeV/c^2
Muon channels							
$W \to \mu\nu$	`wewk8m`	1608588	1960	1.4	—	0.586	
$Z/\gamma^* \to \mu\mu$	`zewk9m`	6701700	355 ± 3	1.4	—	13.5	$M > 20$ GeV/c^2
Both channels							
$Z/\gamma^* \to \tau\tau$	`zewkat`	6849882	238 ± 3	1.4	—	19.0	$M > 30$ GeV/c^2
$t\bar{t}$	`ttop75`	1111652	7.3	—	—	152.3	
WW	`wewkbd`	1596781	1.27	—	—	1.26×10^3	
WZ	`wewkcd`	3598792	0.365	—	0.76	1.19×10^4	
ZZ	`wewkdd`	761342	2.01	—	0.23	1.65×10^3	$M > 15$ GeV/c^2

Table 2: Background expectation and observed number of events for the opposite-sign dilepton events before the Z veto.

	ee	$e\mu$	μe	$\mu\mu$	Total
Fakes	96.9	64.8	55.9	37.4	255.0
Photon-conversions	217.5	-2.3	19.9	—	235.1
Total	314.4 ± 9.7	62.5 ± 4.5	75.8 ± 4.3	37.4 ± 2.7	490.1 ± 14.0
(Stat.)	± 7.4	± 2.3	± 2.8	± 1.1	± 8.9
(Syst.)	± 6.3	± 3.9	± 3.2	± 2.5	± 10.7
$W \rightarrow e\nu$	+0.0	1.3	0.0	0.0	1.3
$Z/\gamma^* \rightarrow ee$	30808.7	+0.0	0.0	0.0	30808.7
$W \rightarrow \mu\nu$	0.0	0.0	+0.0	+0.0	+0.0
$Z/\gamma^* \rightarrow \mu\mu$	0.0	2.2	19.9	25855.2	25877.3
$Z/\gamma^* \rightarrow \tau\tau$	272.9	232.5	279.4	244.0	1028.8
$t\bar{t}$	19.6	13.8	19.0	14.1	66.5
WW	29.0	23.0	30.8	24.8	107.6
WZ	16.6	1.5	1.9	14.7	34.7
ZZ	19.6	0.6	0.8	18.0	39.1
Total MC	31166.4 ± 1892.2	275.0 ± 17.3	351.7 ± 22.1	26170.9 ± 1585.7	57964.0 ± 3497.2
(Stat.)	± 138.8	± 5.0	± 5.2	± 56.0	± 149.8
(Syst.)	± 253.4	± 1.9	± 3.9	± 213.7	± 335.2
(Luminosity)	± 1870.0	± 16.5	± 21.1	± 1570.3	± 3477.8
Fermiophobic higgs (110 GeV/c^2)	0.553 ± 0.034	0.474 ± 0.028	0.552 ± 0.034	0.489 ± 0.030	2.069 ± 0.127
(Stat.)	± 0.007	± 0.006	± 0.007	± 0.006	± 0.013
(Syst.)	± 0.008	± 0.004	± 0.008	± 0.005	± 0.028
(Luminosity)	± 0.033	± 0.028	± 0.033	± 0.029	± 0.124
SM higgs (160 GeV/c^2)	0.187 ± 0.011	0.156 ± 0.009	0.208 ± 0.012	0.174 ± 0.010	0.726 ± 0.044
(Stat.)	± 0.002	± 0.002	± 0.002	± 0.001	± 0.004
(Syst.)	± 0.002	± 0.001	± 0.002	± 0.002	± 0.009
(Luminosity)	± 0.011	± 0.009	± 0.012	± 0.010	± 0.043
Total expected	31480.8 ± 1892.2	337.5 ± 17.9	427.5 ± 22.5	26208.3 ± 1585.7	58454.1 ± 3497.2
Data	28777	338	399	23980	53494

Table 3: Background expectation and observed number of events for the opposite-sign dilepton events after the Z veto.

	ee	$e\mu$	μe	$\mu\mu$	Total
Fakes	94.5	63.2	54.7	36.5	248.9
Photon-conversions	53.7	-2.2	18.2	—	69.7
Total	148.2 ± 6.3	60.9 ± 4.4	72.9 ± 4.2	36.5 ± 2.7	318.5 ± 11.6
(Stat.)	± 4.9	± 2.3	± 2.8	± 1.1	± 6.9
(Syst.)	± 4.0	± 3.8	± 3.1	± 2.4	± 9.4
$W \rightarrow e\nu$	$+0.0$	1.3	0.0	0.0	1.3
$Z/\gamma^* \rightarrow ee$	5621.6	$+0.0$	0.0	0.0	5621.6
$W \rightarrow \mu\nu$	0.0	0.0	$+0.0$	$+0.0$	$+0.0$
$Z/\gamma^* \rightarrow \mu\mu$	0.0	2.1	17.8	5076.6	5096.5
$Z/\gamma^* \rightarrow \tau\tau$	270.3	229.9	276.1	242.0	1018.3
$t\bar{t}$	15.6	11.6	15.2	12.3	54.7
WW	23.8	19.8	25.6	21.7	90.9
WZ	2.0	0.7	0.8	2.3	5.9
ZZ	3.3	0.3	0.4	3.4	7.3
Total MC	5936.6 ± 371.2	265.7 ± 16.8	335.9 ± 21.1	5358.3 ± 325.4	11896.5 ± 723.9
(Stat.)	± 57.6	± 4.9	± 5.1	± 25.1	± 63.2
(Syst.)	± 87.1	± 1.9	± 3.9	± 43.7	± 103.0
(Luminosity)	± 356.2	± 15.9	± 20.2	± 321.5	± 713.8
Fermiophobic higgs (110 GeV/c^2)	0.489 ± 0.030	0.424 ± 0.026	0.490 ± 0.030	0.446 ± 0.027	1.851 ± 0.113
(Stat.)	± 0.007	± 0.006	± 0.006	± 0.006	± 0.013
(Syst.)	± 0.007	± 0.004	± 0.008	± 0.005	± 0.025
(Luminosity)	± 0.029	± 0.025	± 0.029	± 0.026	± 0.110
SM higgs (160 GeV/c^2)	0.159 ± 0.009	0.137 ± 0.008	0.187 ± 0.010	0.157 ± 0.009	0.635 ± 0.038
(Stat.)	± 0.002	± 0.001	± 0.002	± 0.001	± 0.003
(Syst.)	± 0.002	± 0.001	± 0.002	± 0.001	± 0.008
(Luminosity)	± 0.009	± 0.008	± 0.010	± 0.009	± 0.038
Total expected	6084.8 ± 371.2	326.7 ± 17.4	408.8 ± 21.6	5394.8 ± 325.4	12215.0 ± 724.0
Data	5731	327	386	4908	11352

Table 4: Background expectation and observed number of events for the like-sign dilepton events before the Z veto.

	ee	$e\mu$	μe	$\mu\mu$	Total
Fakes	79.8	50.2	39.0	24.8	193.9
Photon-conversions	36.2	-0.2	26.9	—	62.9
Total	116.1 ± 6.7	50.0 ± 2.8	65.9 ± 4.7	24.8 ± 1.6	256.8 ± 10.2
(Stat.)	± 5.7	± 2.3	± 4.0	± 0.9	± 8.0
(Syst.)	± 3.5	± 1.6	± 2.5	± 1.3	± 6.4
$W \rightarrow e\nu$	$+0.00$	$+0.00$	0.00	0.00	$+0.00$
$Z/\gamma^* \rightarrow ee$	$+0.00$	$+0.00$	0.00	0.00	$+0.00$
$W \rightarrow \mu\nu$	0.00	$+0.00$	$+0.00$	$+0.00$	$+0.00$
$Z/\gamma^* \rightarrow \mu\mu$	0.00	$+0.00$	0.12	0.12	0.25
$Z/\gamma^* \rightarrow \tau\tau$	$+0.00$	$+0.00$	$+0.00$	$+0.00$	$+0.00$
$t\bar{t}$	$+0.00$	0.01	$+0.00$	$+0.00$	0.01
WW	$+0.00$	$+0.00$	$+0.00$	0.00	$+0.00$
WZ	1.71	1.40	1.75	1.46	6.32
ZZ	0.53	0.49	0.59	0.49	2.10
Total MC	2.24 ± 0.14	1.90 ± 0.12	2.46 ± 0.19	2.08 ± 0.18	8.68 ± 0.55
(Stat.)	± 0.03	± 0.03	± 0.12	± 0.13	± 0.18
(Syst.)	± 0.02	± 0.01	± 0.02	± 0.02	± 0.05
(Luminosity)	± 0.13	± 0.11	± 0.15	± 0.12	± 0.52
Fermiophobic higgs (110 GeV/c^2)	0.322 ± 0.020	0.275 ± 0.016	0.334 ± 0.021	0.290 ± 0.017	1.222 ± 0.075
(Stat.)	± 0.005	± 0.005	± 0.005	± 0.005	± 0.010
(Syst.)	± 0.004	± 0.002	± 0.005	± 0.003	± 0.016
(Luminosity)	± 0.019	± 0.016	± 0.020	± 0.017	± 0.073
SM higgs (160 GeV/c^2)	0.093 ± 0.005	0.075 ± 0.004	0.104 ± 0.006	0.089 ± 0.005	0.362 ± 0.021
(Stat.)	± 0.001	± 0.001	± 0.001	± 0.001	± 0.002
(Syst.)	± 0.001	± 0.001	± 0.001	± 0.001	± 0.004
(Luminosity)	± 0.005	± 0.004	± 0.006	± 0.005	± 0.021
Total expected	118.3 ± 6.7	51.9 ± 2.8	68.3 ± 4.7	26.9 ± 1.6	265.4 ± 10.2
Data	121	45	69	22	257

Table 5: Background expectation and observed number of events for the like-sign dilepton events after the Z veto.

	ee	$e\mu$	μe	$\mu\mu$	Total
Fakes	77.1	48.5	37.7	23.9	187.2
Photon-conversions	30.0	-0.2	26.3	—	56.0
Total	107.1 ± 6.5	48.3 ± 2.7	64.0 ± 4.6	23.9 ± 1.5	243.2 ± 10.0
(Stat.)	± 5.6	± 2.3	± 4.0	± 0.9	± 7.9
(Syst.)	± 3.3	± 1.5	± 2.4	± 1.2	± 6.1
$W \to e\nu$	+0.00	+0.00	0.00	0.00	+0.00
$Z/\gamma^* \to ee$	+0.00	+0.00	0.00	0.00	+0.00
$W \to \mu\nu$	0.00	+0.00	+0.00	+0.00	+0.00
$Z/\gamma^* \to \mu\mu$	0.00	+0.00	0.12	0.12	0.25
$Z/\gamma^* \to \tau\tau$	+0.00	+0.00	+0.00	+0.00	+0.00
$t\bar{t}$	+0.00	0.01	+0.00	+0.00	0.01
WW	+0.00	+0.00	+0.00	0.00	+0.00
WZ	0.48	0.67	0.79	0.79	2.73
ZZ	0.08	0.13	0.15	0.16	0.53
Total MC	0.56 ± 0.04	0.82 ± 0.05	1.07 ± 0.14	1.07 ± 0.14	3.52 ± 0.28
(Stat.)	± 0.01	± 0.02	± 0.12	± 0.13	± 0.18
(Syst.)	± 0.01	± 0.00	± 0.01	± 0.01	± 0.02
(Luminosity)	± 0.03	± 0.05	± 0.06	± 0.06	± 0.21
Fermiophobic higgs (110 GeV/c^2)	0.274 ± 0.017	0.269 ± 0.016	0.330 ± 0.020	0.253 ± 0.015	1.127 ± 0.069
(Stat.)	± 0.005	± 0.005	± 0.005	± 0.004	± 0.010
(Syst.)	± 0.004	± 0.002	± 0.005	± 0.002	± 0.015
(Luminosity)	± 0.016	± 0.016	± 0.019	± 0.015	± 0.067
SM higgs (160 GeV/c^2)	0.076 ± 0.004	0.073 ± 0.004	0.100 ± 0.006	0.075 ± 0.004	0.326 ± 0.019
(Stat.)	± 0.001	± 0.001	± 0.001	± 0.001	± 0.002
(Syst.)	± 0.001	± 0.001	± 0.001	± 0.001	± 0.004
(Luminosity)	± 0.004	± 0.004	± 0.006	± 0.004	± 0.019
Total expected	107.6 ± 6.5	49.1 ± 2.7	65.0 ± 4.6	25.0 ± 1.5	246.7 ± 10.0
Data	101	45	64	20	230

Table 6: Background expectation and observed number of events for the opposite-sign dilepton events before the Z veto. The silicon-hit requirement for tracks is imposed.

	ee	$e\mu$	μe	$\mu\mu$	Total
Fakes	64.1	44.2	46.4	31.7	186.4
Photon-conversions	137.7	0.3	6.7	—	144.7
Total	201.8 ± 7.8	44.5 ± 3.6	53.1 ± 3.2	31.7 ± 2.4	331.1 ± 11.3
(Stat.)	± 4.7	± 1.5	± 2.0	± 1.0	± 6.0
(Syst.)	± 6.2	± 3.3	± 2.6	± 2.2	± 9.6
$W \to e\nu$	+0.0	1.3	0.0	0.0	1.3
$Z/\gamma^* \to ee$	24613.5	+0.0	0.0	0.0	24613.5
$W \to \mu\nu$	0.0	0.0	+0.0	+0.0	+0.0
$Z/\gamma^* \to \mu\mu$	0.0	1.8	15.3	20227.9	20243.5
$Z/\gamma^* \to \tau\tau$	210.5	177.3	214.8	186.7	788.4
$t\bar{t}$	15.4	10.7	15.3	11.1	52.5
WW	21.7	17.5	23.2	18.9	81.3
WZ	13.1	1.2	1.5	11.7	27.5
ZZ	15.5	0.5	0.7	14.5	31.1
Total MC	24889.8 ± 1511.9	210.3 ± 13.4	270.7 ± 17.1	20468.4 ± 1240.2	45839.1 ± 2766.1
(Stat.)	± 120.8	± 4.3	± 4.4	± 48.2	± 130.3
(Syst.)	± 202.5	± 1.4	± 3.0	± 166.0	± 264.7
(Luminosity)	± 1493.4	± 12.6	± 16.2	± 1228.1	± 2750.4
Fermiophobic higgs	0.463 ± 0.028	0.399 ± 0.024	0.465 ± 0.029	0.416 ± 0.029	1.744 ± 0.107
(110 GeV/c^2)					
(Stat.)	± 0.006	± 0.006	± 0.006	± 0.006	± 0.012
(Syst.)	± 0.008	± 0.004	± 0.008	± 0.005	± 0.026
(Luminosity)	± 0.027	± 0.024	± 0.029	± 0.025	± 0.107
SM higgs	0.156 ± 0.009	0.132 ± 0.007	0.173 ± 0.010	0.147 ± 0.008	0.609 ± 0.037
(160 GeV/c^2)					
(Stat.)	± 0.002	± 0.001	± 0.002	± 0.001	± 0.003
(Syst.)	± 0.002	± 0.001	± 0.002	± 0.001	± 0.008
(Luminosity)	± 0.009	± 0.007	± 0.010	± 0.008	± 0.036
Total expected	25091.5 ± 1511.9	254.7 ± 13.9	323.8 ± 17.4	20500.1 ± 1240.2	46170.1 ± 2766.1
Data	23773	270	314	20083	44440

Table 7: Background expectation and observed number of events for the opposite-sign dilepton events after the Z veto. The silicon-hit requirement for tracks is imposed.

	ee	$e\mu$	μe	$\mu\mu$	Total
Fakes	61.9	42.7	45.5	31.1	181.2
Photon-conversions	29.1	0.3	6.3	—	35.6
Total	91.0 ± 4.4	43.0 ± 3.5	51.8 ± 3.2	31.1 ± 2.4	216.8 ± 9.2
(Stat.)	± 3.0	± 1.4	± 1.9	± 1.0	± 4.8
(Syst.)	± 3.3	± 3.2	± 2.5	± 2.2	± 7.8
$W \rightarrow e\nu$	+0.0	1.3	0.0	0.0	1.3
$Z/\gamma^* \rightarrow ee$	4493.6	+0.0	0.0	0.0	4493.6
$W \rightarrow \mu\nu$	0.0	0.0	+0.0	+0.0	+0.0
$Z/\gamma^* \rightarrow \mu\mu$	0.0	1.7	13.5	3968.2	3983.4
$Z/\gamma^* \rightarrow \tau\tau$	208.4	175.5	211.9	184.1	779.9
$t\bar{t}$	12.4	8.9	12.2	9.6	43.1
WW	17.9	15.1	19.2	16.6	68.7
WZ	1.6	0.6	0.6	1.8	4.6
ZZ	2.6	0.2	0.3	2.7	5.8
Total MC	4736.5 ± 296.8	203.2 ± 13.0	257.7 ± 16.3	4183.1 ± 254.2	9380.5 ± 571.3
(Stat.)	± 50.2	± 4.2	± 4.4	± 21.6	± 55.0
(Syst.)	± 69.3	± 1.4	± 2.9	± 33.9	± 81.3
(Luminosity)	± 284.2	± 12.2	± 15.5	± 251.0	± 562.8
Fermiophobic higgs (110 GeV/c^2)	0.411 ± 0.025	0.358 ± 0.021	0.412 ± 0.025	0.379 ± 0.027	1.562 ± 0.093
(Stat.)	± 0.006	± 0.005	± 0.006	± 0.005	± 0.012
(Syst.)	± 0.007	± 0.004	± 0.007	± 0.004	± 0.024
(Luminosity)	± 0.024	± 0.021	± 0.024	± 0.027	± 0.090
SM higgs (160 GeV/c^2)	0.132 ± 0.007	0.115 ± 0.006	0.152 ± 0.009	0.133 ± 0.007	0.533 ± 0.031
(Stat.)	± 0.001	± 0.001	± 0.001	± 0.001	± 0.003
(Syst.)	± 0.002	± 0.001	± 0.002	± 0.001	± 0.007
(Luminosity)	± 0.007	± 0.006	± 0.009	± 0.007	± 0.031
Total expected	4827.5 ± 296.8	246.2 ± 13.5	309.5 ± 16.6	4214.1 ± 254.2	9597.3 ± 571.4
Data	4730	261	306	4098	9395

Table 8: Background expectation and observed number of events for the like-sign dilepton events before the Z veto. The silicon-hit requirement for tracks is imposed.

	ee	$e\mu$	μe	$\mu\mu$	Total
Fakes	48.4	31.4	31.3	20.4	131.4
Photon-conversions	8.4	-0.4	6.4	—	14.4
Total	56.8 ± 3.4	31.0 ± 1.9	37.7 ± 2.6	20.4 ± 1.4	145.9 ± 6.3
(Stat.)	± 2.4	± 1.3	± 1.9	± 0.8	± 4.2
(Syst.)	± 2.3	± 1.4	± 1.8	± 1.1	± 4.7
$W \rightarrow e\nu$	+0.00	+0.00	0.00	0.00	+0.00
$Z/\gamma^* \rightarrow ee$	+0.00	+0.00	0.00	0.00	+0.00
$W \rightarrow \mu\nu$	0.00	0.00	+0.00	+0.00	+0.00
$Z/\gamma^* \rightarrow \mu\mu$	0.00	+0.00	0.12	0.12	0.23
$Z/\gamma^* \rightarrow \tau\tau$	+0.00	+0.00	+0.00	+0.00	+0.00
$t\bar{t}$	+0.00	0.01	+0.00	+0.00	0.01
WW	+0.00	0.00	+0.00	0.00	+0.00
WZ	1.35	1.11	1.39	1.18	5.03
ZZ	0.43	0.41	0.49	0.40	1.74
Total MC	1.78 ± 0.11	1.54 ± 0.10	2.00 ± 0.17	1.70 ± 0.16	7.02 ± 0.46
(Stat.)	± 0.03	± 0.03	± 0.12	± 0.12	± 0.17
(Syst.)	± 0.02	± 0.01	± 0.02	± 0.01	± 0.04
(Luminosity)	± 0.11	± 0.09	± 0.12	± 0.10	± 0.42
Fermiophobic higgs (110 GeV/c^2)	0.268 ± 0.017	0.230 ± 0.013	0.275 ± 0.017	0.245 ± 0.014	1.019 ± 0.063
(Stat.)	± 0.005	± 0.004	± 0.005	± 0.004	± 0.009
(Syst.)	± 0.004	± 0.002	± 0.004	± 0.003	± 0.015
(Luminosity)	± 0.016	± 0.013	± 0.017	± 0.014	± 0.063
SM higgs (160 GeV/c^2)	0.077 ± 0.004	0.063 ± 0.004	0.087 ± 0.005	0.076 ± 0.004	0.303 ± 0.018
(Stat.)	± 0.001	± 0.001	± 0.001	± 0.001	± 0.002
(Syst.)	± 0.001	± 0.001	± 0.001	± 0.001	± 0.004
(Luminosity)	± 0.004	± 0.004	± 0.005	± 0.004	± 0.018
Total expected	58.6 ± 3.4	32.5 ± 1.9	39.7 ± 2.6	22.1 ± 1.4	152.9 ± 6.3
Data	61	26	43	18	148

Table 9: Background expectation and observed number of events for the like-sign dilepton events after the Z veto. The silicon-hit requirement for tracks is imposed.

	ee	$e\mu$	μe	$\mu\mu$	Total
Fakes	46.1	29.8	30.4	19.8	126.1
Photon-conversions	6.2	-0.4	6.4	—	12.2
Total	52.3 ± 6.9	29.4 ± 4.0	36.8 ± 5.1	19.7 ± 3.1	138.3 ± 9.2
(Stat.)	± 2.2	± 1.2	± 1.7	± 0.8	± 3.1
(Syst.)	± 6.2	± 3.8	± 4.8	± 3.0	± 8.7
$W \rightarrow e\nu$	$+0.00$	$+0.00$	0.00	0.00	$+0.00$
$Z/\gamma^* \rightarrow ee$	$+0.00$	$+0.00$	0.00	0.00	$+0.00$
$W \rightarrow \mu\nu$	0.00	0.00	$+0.00$	$+0.00$	$+0.00$
$Z/\gamma^* \rightarrow \mu\mu$	0.00	$+0.00$	0.09	0.09	0.18
$Z/\gamma^* \rightarrow \tau\tau$	$+0.00$	$+0.00$	$+0.00$	$+0.00$	$+0.00$
$t\bar{t}$	$+0.00$	0.01	$+0.00$	$+0.00$	0.01
WW	$+0.00$	0.00	$+0.00$	0.00	$+0.00$
WZ	0.39	0.55	0.66	0.67	2.26
ZZ	0.07	0.10	0.13	0.15	0.32
Total MC	0.46 ± 0.03	0.66 ± 0.06	0.88 ± 0.11	0.91 ± 0.11	2.86 ± 0.37
(Stat.)	± 0.01	± 0.02	± 0.09	± 0.09	± 0.13
(Syst.)	± 0.03	± 0.03	± 0.05	± 0.04	± 0.07
(Luminosity)	± 0.03	± 0.04	± 0.05	± 0.05	± 0.17
Fermiophobic higgs	0.227 ± 0.013	0.224 ± 0.013	0.271 ± 0.016	0.214 ± 0.012	0.938 ± 0.050
(110 GeV/c^2)					
(Stat.)	± 0.004	± 0.004	± 0.004	± 0.004	± 0.009
(Syst.)	± 0.003	± 0.002	± 0.002	± 0.004	± 0.014
(Luminosity)	± 0.013	± 0.013	± 0.016	± 0.012	± 0.050
SM higgs	0.063 ± 0.003	0.061 ± 0.003	0.084 ± 0.005	0.064 ± 0.003	0.272 ± 0.016
(160 GeV/c^2)					
(Stat.)	± 0.001	± 0.001	± 0.001	± 0.001	± 0.002
(Syst.)	± 0.001	± 0.001	± 0.001	± 0.001	± 0.003
(Luminosity)	± 0.003	± 0.003	± 0.005	± 0.003	± 0.016
Total expected	52.8 ± 6.6	30.6 ± 4.0	37.6 ± 5.1	20.7 ± 3.1	141.7 ± 9.2
Data	51	26	41	16	134

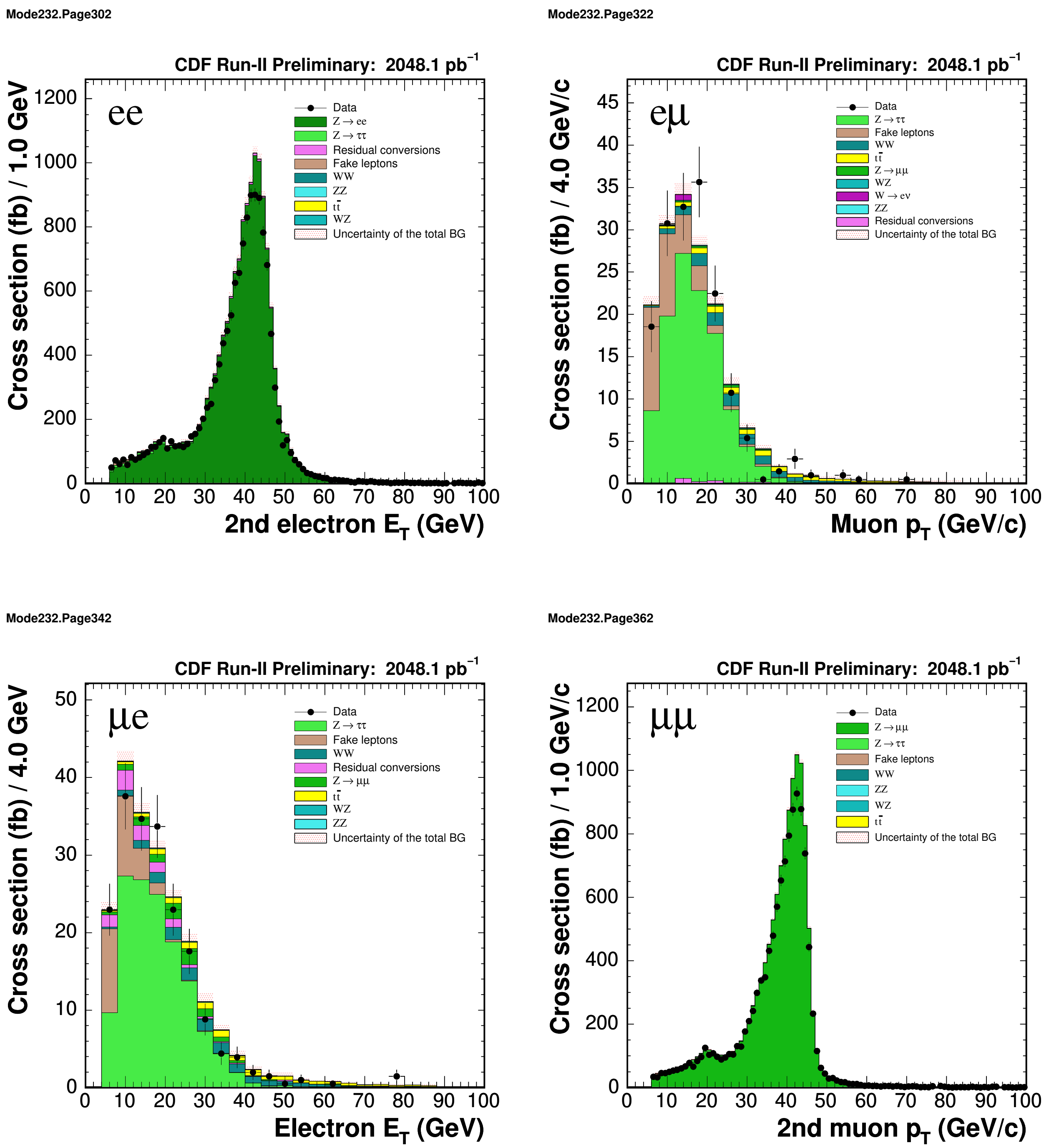

Figure 1: Comparison of the 2nd lepton p_T or E_T distributions between the data and the background prediction for the opposite-sign dilepton events before the Z veto.

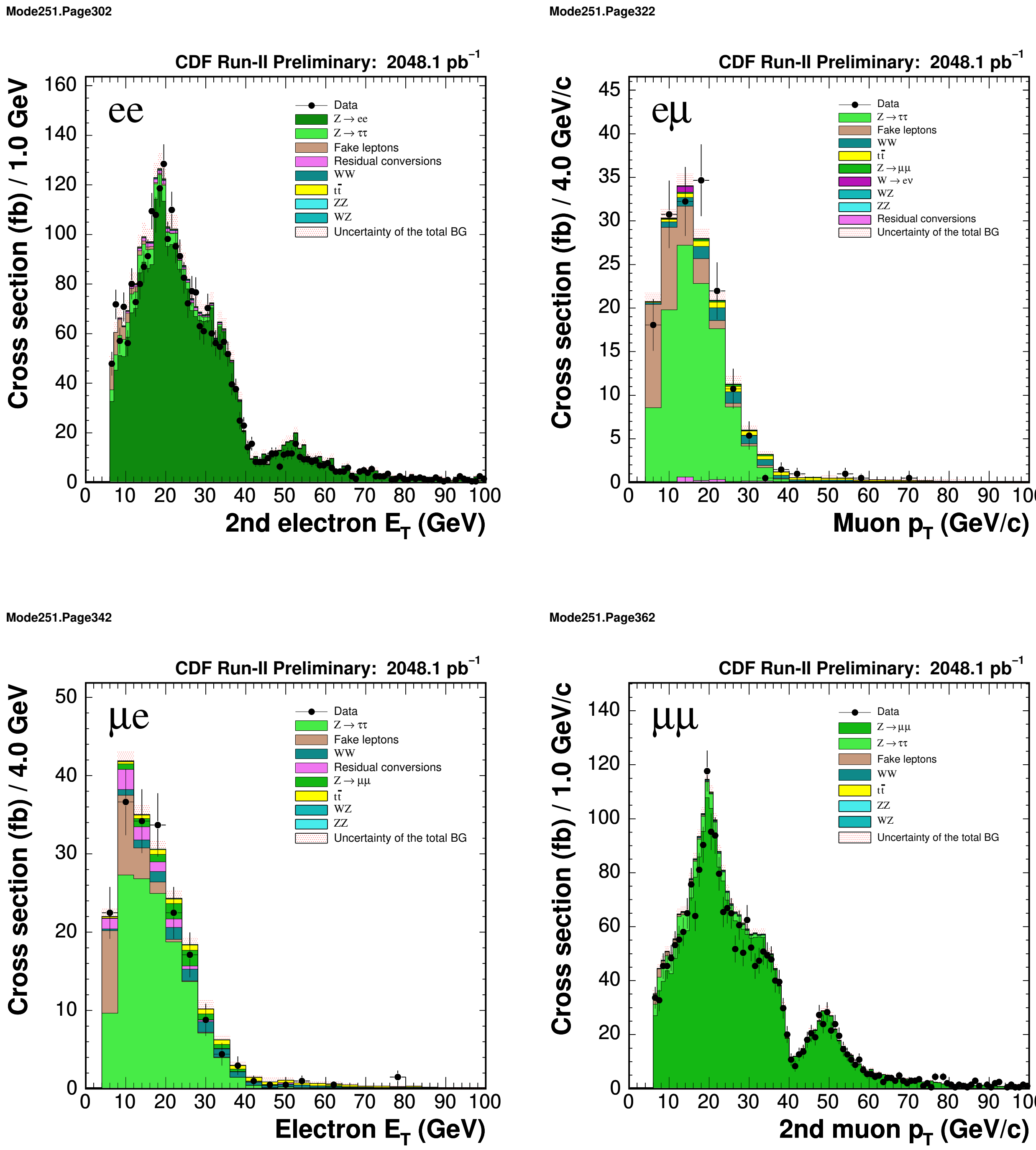

Figure 2: Comparison of the 2nd lepton p_T or E_T distributions between the data and the background prediction for the opposite-sign dilepton events after the Z veto.

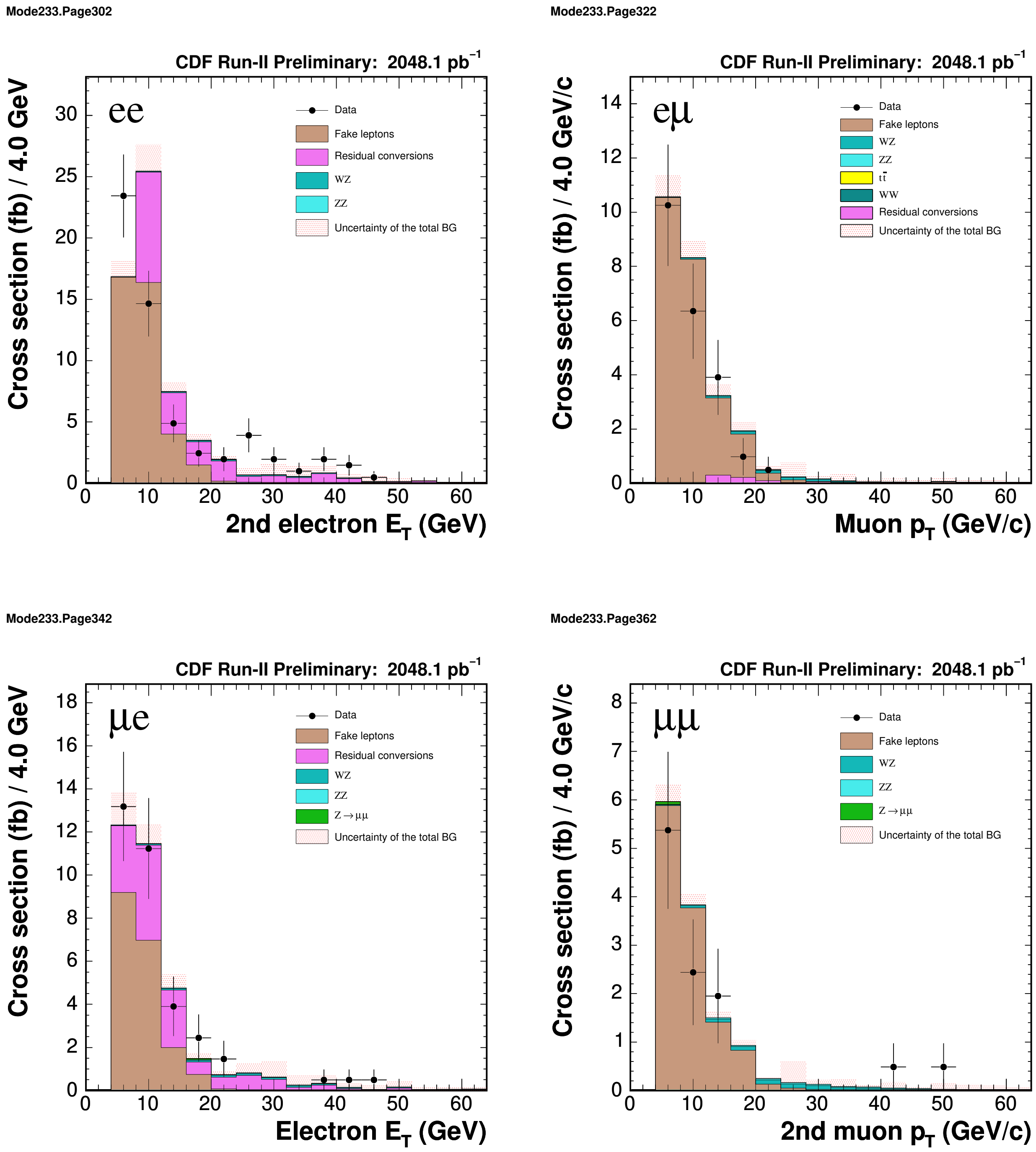

Figure 3: Comparison of the 2nd lepton p_T or E_T distributions between the data and the background prediction for the like-sign dilepton events before the Z veto.

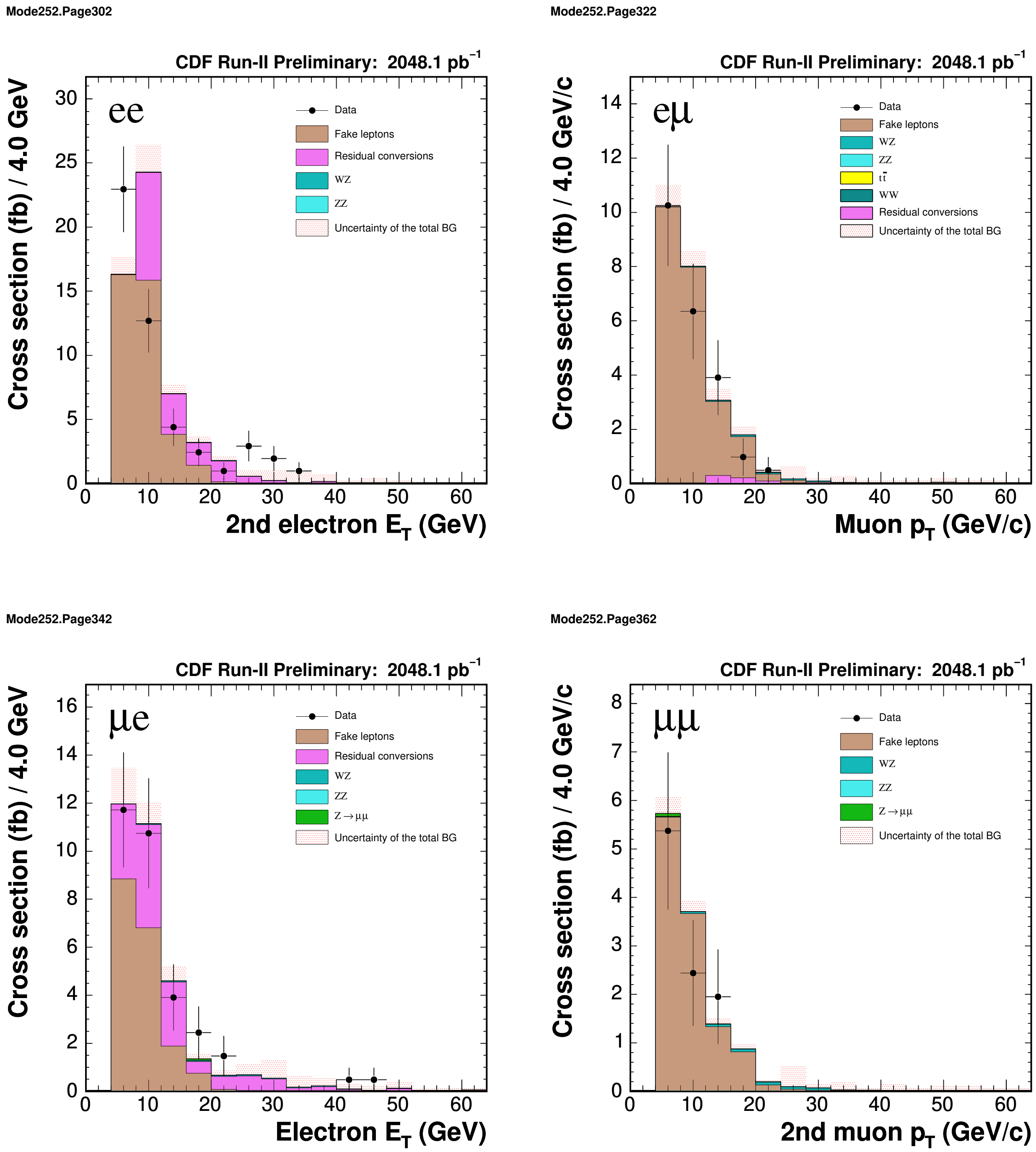

Figure 4: Comparison of the 2nd lepton p_T or E_T distributions between the data and the background prediction for the like-sign dilepton events after the Z veto.

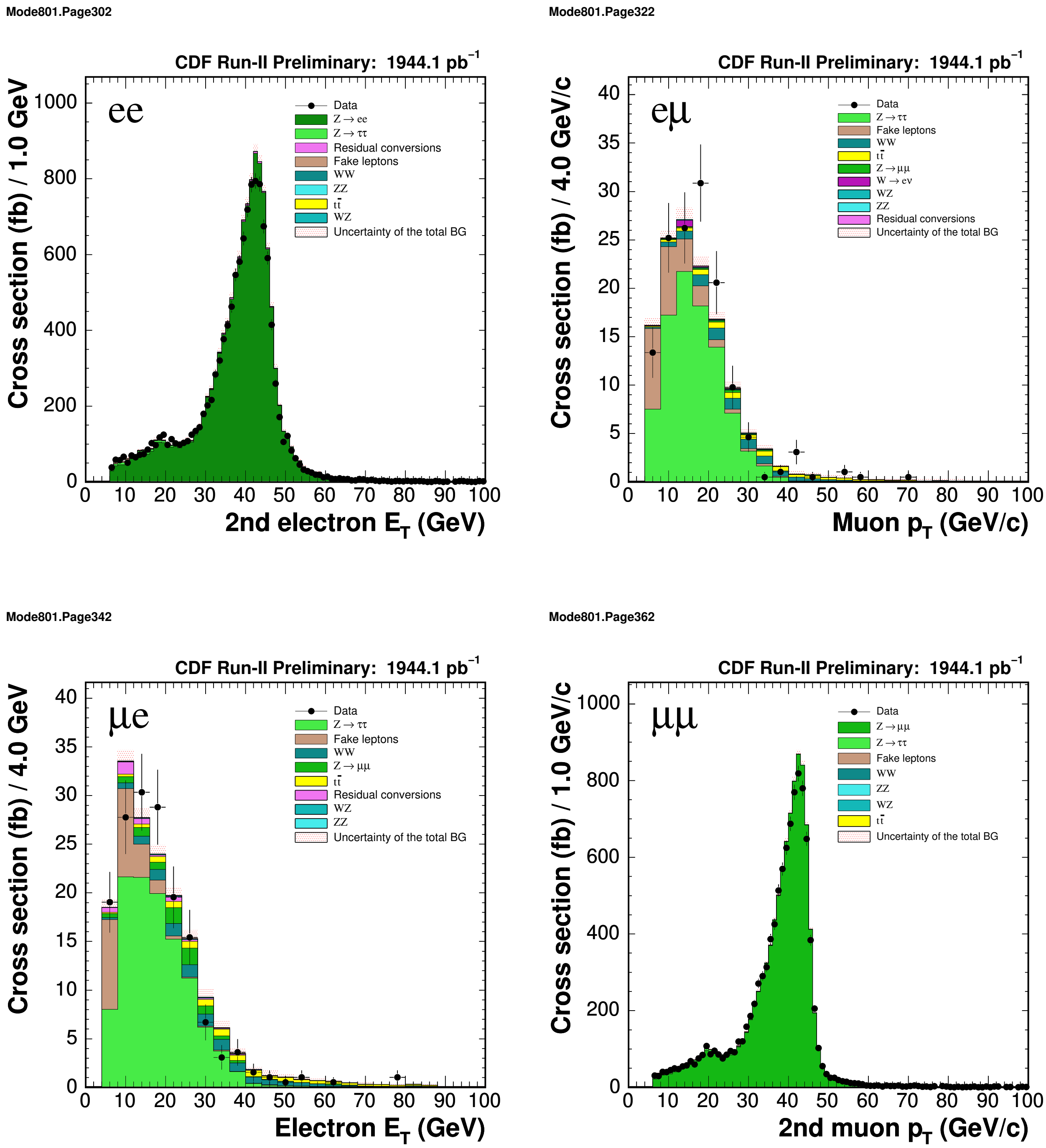

Figure 5: Comparison of the 2nd lepton p_T or E_T distributions between the data and the background prediction for the opposite-sign dilepton events before the Z veto. The silicon-hit requirement for tracks is imposed.

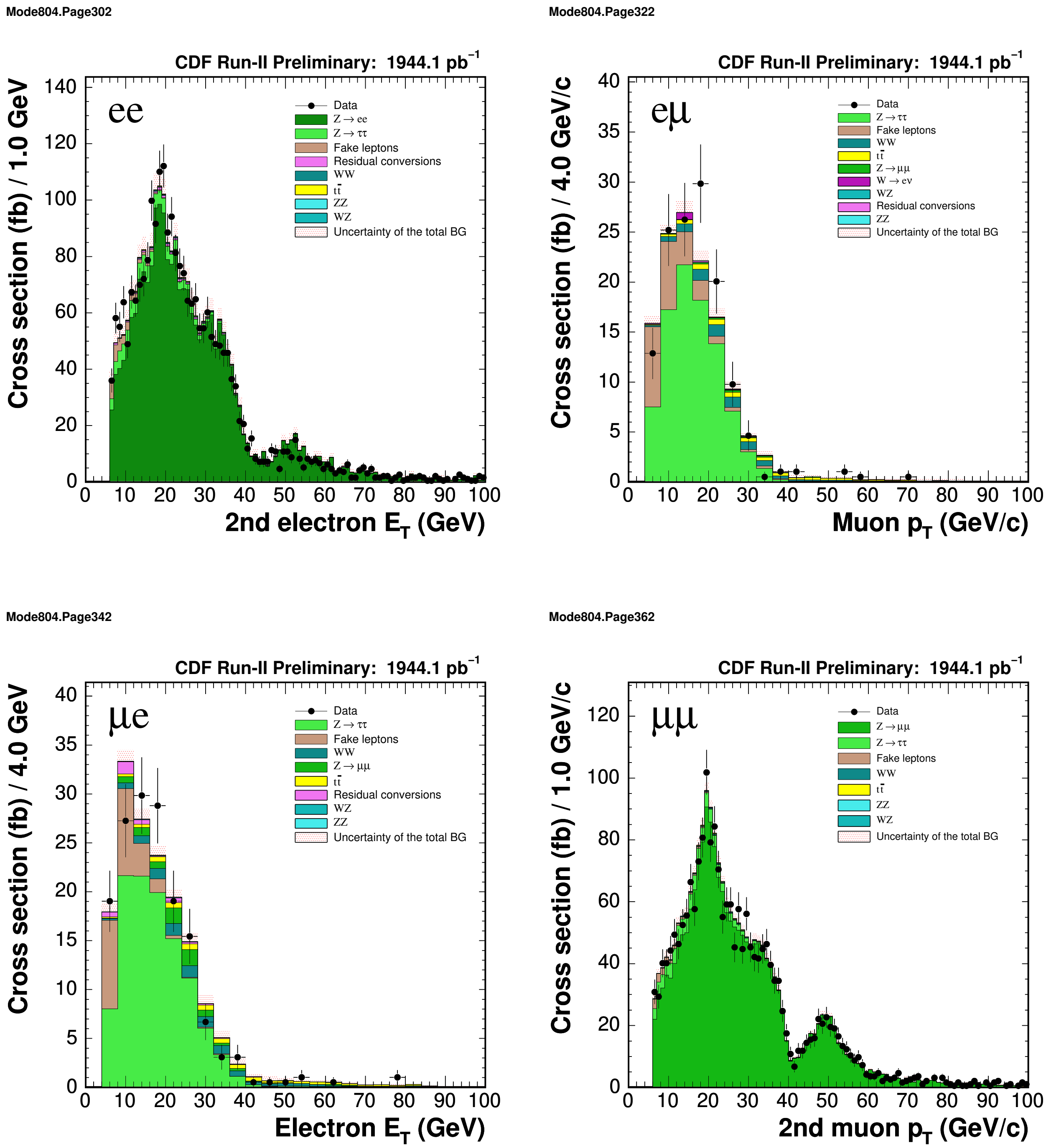

Figure 6: Comparison of the 2nd lepton p_T or E_T distributions between the data and the background prediction for the opposite-sign dilepton events after the Z veto. The silicon-hit requirement for tracks is imposed.

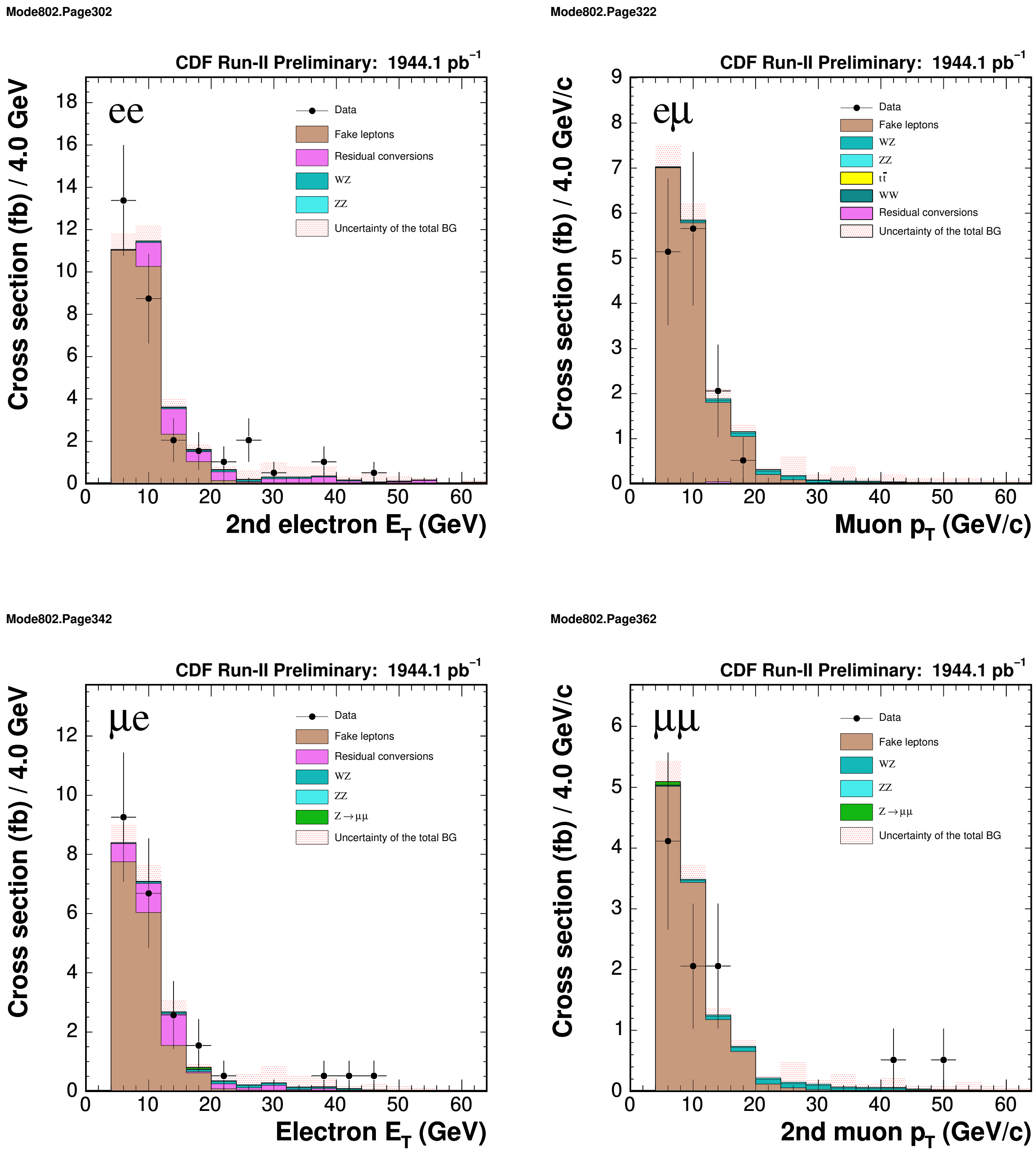

Figure 7: Comparison of the 2nd lepton p_T or E_T distributions between the data and the background prediction for the like-sign dilepton events before the Z veto. The silicon-hit requirement for tracks is imposed.

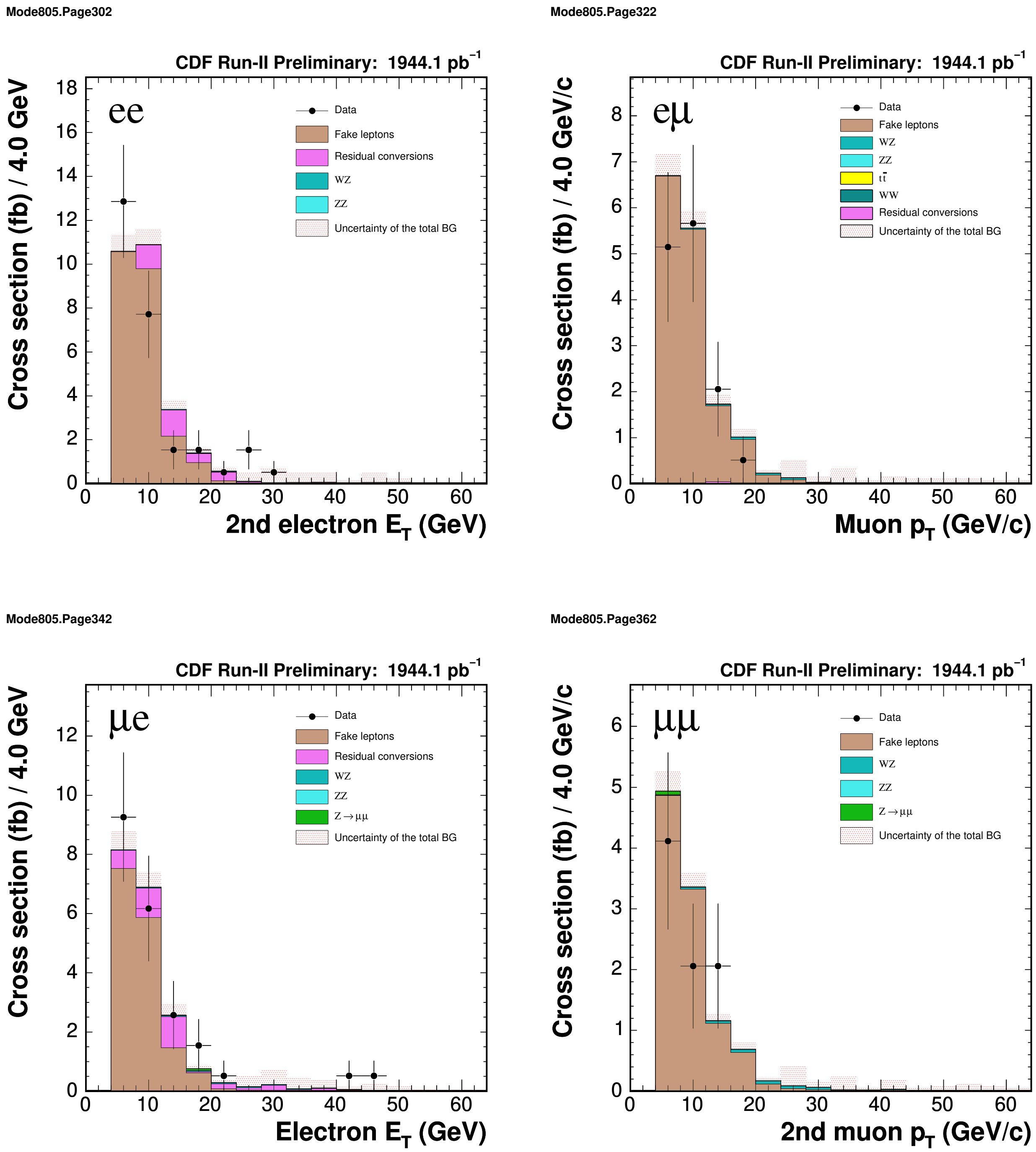

Figure 8: Comparison of the 2nd lepton p_T or E_T distributions between the data and the background prediction for the like-sign dilepton events after the Z veto. The silicon-hit requirement for tracks is imposed.

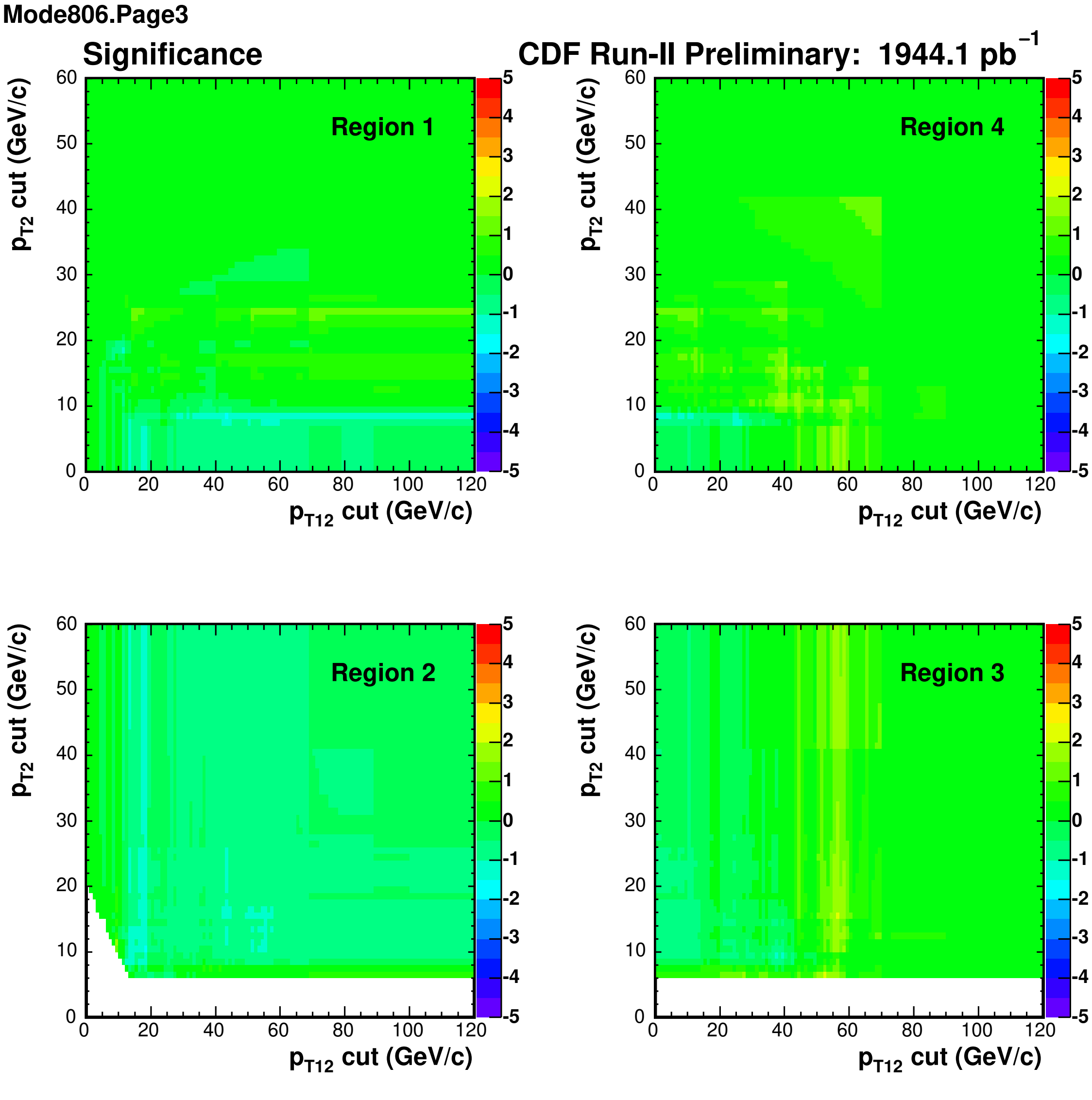

Figure 9: Significance of the number of observed like-sign data with respect to the background prediction as a function of cut values on the 2nd lepton p_T and the p_T of the dilepton system after the Z veto. The region 1 represents the upper-left region when we divide the plane into 4 regions for a given set of cut values, the region 2 is the lower-left, the region 3 is the lower-right, and the region 4 is the upper-right. The silicon-hit requirement for tracks is imposed.

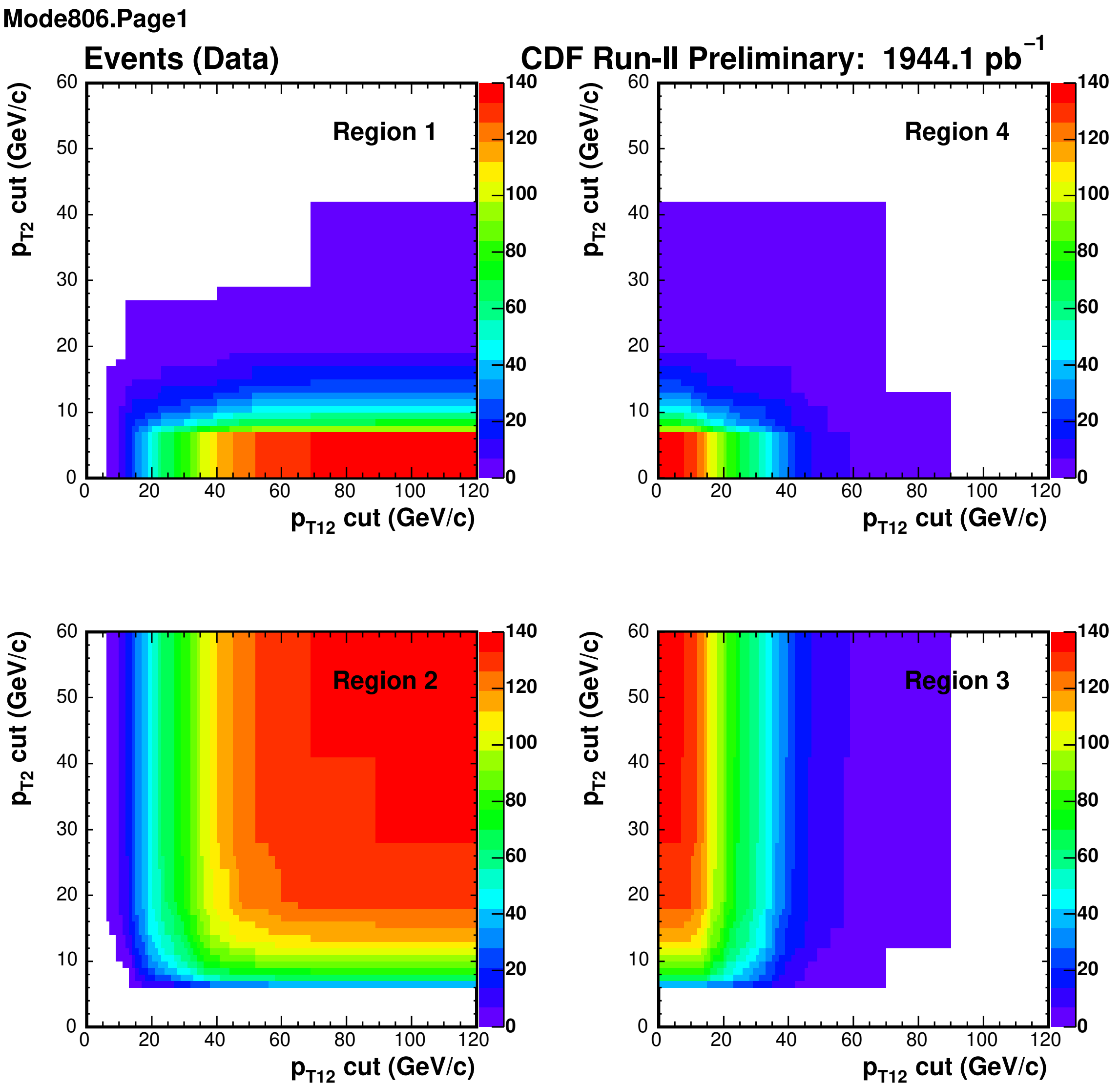

Figure 10: The number of like-sign dilepton events observed in the data as a function of cut values on the 2nd lepton p_T and the p_T of the dilepton system after the Z veto. The region 1 represents the upper-left region when we divide the plane into 4 regions for a given set of cut values, the region 2 is the lower-left, the region 3 is the lower-right, and the region 4 is the upper-right. The silicon-hit requirement for tracks is imposed.

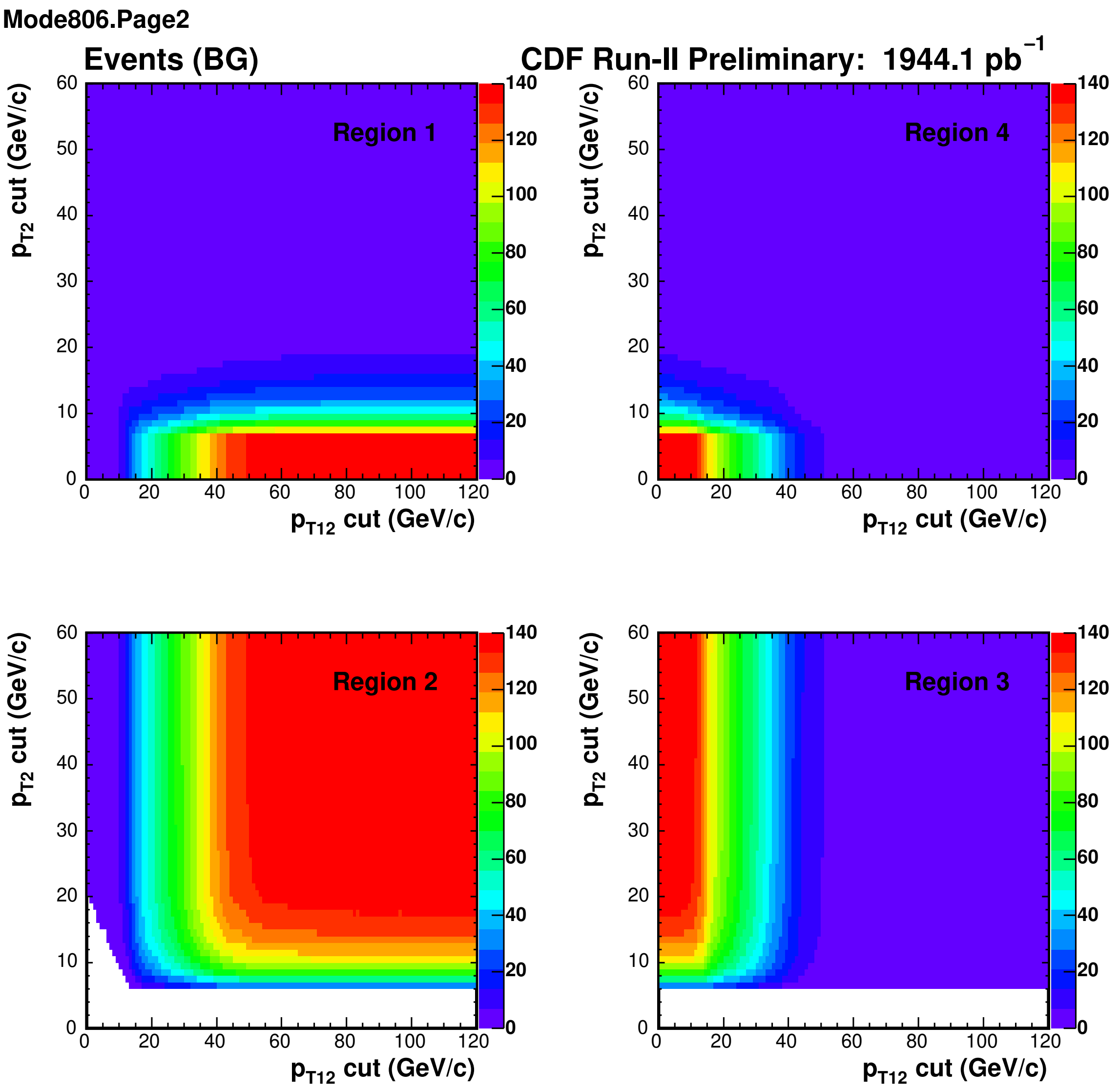

Figure 11: The background prediction of the number of like-sign dilepton events as a function of cut values on the 2nd lepton p_T and the p_T of the dilepton system after the Z veto. The region 1 represents the upper-left region when we divide the plane into 4 regions for a given set of cut values, the region 2 is the lower-left, the region 3 is the lower-right, and the region 4 is the upper-right. The silicon-hit requirement for tracks is imposed.

References

[1] Hirokazu Kobayashi, Kazuhiro Yamamoto, and Yoshihiro Seiya, "Background Estimation for High-p_T Like-Sign Dilepton Analysis", CDF7261 (Version 1.0).

[2] Hirokazu Kobayashi, Kazuhiro Yamamoto, and Yoshihiro Seiya, "Search for the WH Production Using High-p_T Isolated Like-Sign Dilepton Events in Run II", CDF7262 (Version 1.0).

[3] Toru Okusawa, Yoshihiro Seiya, Takayuki Wakisaka, and Kazuhiro Yamamoto, "Baseline Selection of High-p_T Dilepton Events to Search for the Wh Production", CDF7260 (Version 2.0).

[4] Toru Okusawa, Yoshihiro Seiya, Takayuki Wakisaka, and Kazuhiro Yamamoto, "Study of Conversion Detection Efficiency for the High-p_T Like-Sign Dilepton Analysis to Search for the Wh Production", CDF8078 (Version 2.0).

[5] Toru Okusawa, Yoshihiro Seiya, Takayuki Wakisaka, and Kazuhiro Yamamoto, "Study of Fake-Lepton Rates for the High-p_T Like-Sign Dilepton Analysis to Search for the Wh Production", CDF9239 (Version 2.0).

[6] Toru Okusawa, Yoshihiro Seiya, Takayuki Wakisaka, and Kazuhiro Yamamoto, "Estimation of Monte-Carlo Scale Factors for the High-p_T Like-Sign Dilepton Analysis to Search for the Wh Production", CDF9238 (Version 2.0).

[7] Craig Blocker, John Conway, Luc Demortier, Joel Heinrich, Tom Junk, Louis Lyons, and Giovanni Punzi, "Simple Facts about P-Values", CDF8023.